ACES Asian Chemical Editorial Society

DOI: 10.1002/asia.201900024

CHEMISTRY AN ASIAN JOURNAL Communication

Preferential Face-on and Edge-on Orientation of Thiophene Oligomers by Rational Molecular Design

Tanwistha Ghosh,[a, b] Shinji Nagasawa,[c] Neethi Raveendran,[a] Vibhu Darshan,[a] Akinori Saeki,[c] and Vijayakumar C. Nair*[a, b]

Abstract: Precise control over the supramolecular organization of organic semiconducting materials guiding to exclusive face-on or edge-on orientation is a challenging task. In the present work, we study the preferential packing of thiophene oligomers induced through rational molecular designing and self-assembly. The acceptor–donor–acceptor-type oligomers having 2-(1,1-dicyano-methylene)rhodanine as acceptor (**OT1**) favored a face-on packing, whereas that of functionalized with *N*-octyl rhodanine (**OT2**) preferred an edge-on packing as evident from 2D-grazing incidence angle X-ray diffraction, tapping-mode atomic force microscopy (AFM) and Raman spectroscopy analyses. The oligomers exhibited anisotropic conductivity in the self-assembled state as an outcome of the preferred orientation, revealed by the conducting AFM experiment.

Excogitation of organic semiconducting materials with precise film-state packing is an important task in organic electronics as the organization of molecules plays a crucial role on the charge transport properties of materials thus influencing their optoelectronic functions and device performance. It is established that face-on packing of oligomers/polymers with respect to the substrate is advantageous for photovoltaic device application, whereas, edge-on packing is suitable for transistors.[1] In literature, various methods have been reported to orient organic semiconductors in a particular direction onto the substrate. Rational design of the basic molecular structure using different alkyl chains and pi-aromatic units to provide a pre-programmed architecture is considered as the most effective approach towards this end.[2] Other methods include the selection of solvents,[3] use of solvent additives,[4] and thermal and/or solvent vapor annealing of the films.[5]

DeLongchamp and McCulloch reported the transition in molecular packing from a preferentially edge-on to face-on orientation with the increase in density of the attached side chains.[6] Jenekhe and co-workers have demonstrated that by varying the length of the alkyl side chain on the backbone of thiazolothiazole-dithienosilole copolymer, preferential orientation could be achieved.[7] They have introduced linear as well as branched alkyl chains on the backbone of a co-polymer; the latter exhibited face-on orientation and resulted in better performance in the solar cell. Osaka et al. have reported a co-polymer comprising of naphthodithiophene and napthobis-[1,2,5]thiadiazole; alkylation of the backbone with 2-hexyldecyl resulted in an edge-on orientation and with that of 2-decyltetradecyl yielded a face-on orientation.[8] The influences by bringing in structural modifications are, by far, studied mostly in polymers and not much in oligomers. However, oligomers are finding special attention for organic device applications in recent years as they are relatively easy to synthesize in high purity, better batch-to-batch reproducibility and easy functionalization compared to their polymer counterparts. Hence it is important to study the packing control through molecular engineering in semiconducting oligomers for developing efficient functional electronic devices.

Herein, we report the synthesis and study of two acceptor-donor-acceptor (A-D-A) type oligothiophene derivatives, **OT1** and **OT2**. The central part of both oligomers is a thienothiophene, which is flanked by dioctyl terthiophenes on either side and an acceptor, 2-(1,1-dicyanomethylene)rhodanine (**OT1**) or *N*-octyl rhodanine (**OT2**; Scheme 1). Notably, we found that **OT1** comprised of unequal length of the alkyl chain (and unequal chain density) on the pi-conjugated backbone and acceptor is stacking parallel to the substrate resulting in face-on orientation of the oligomers. On the other hand, **OT2** with equal length of alkyl chains on thiophene as well as on the acceptor is stacking perpendicular to the substrate, resulting in an edge-on orientation. The molecular structures of **OT1** and **OT2** along with a simplified schematic representation of the stacking of oligomers in the film state are shown in Scheme 1.

The oligomers were synthesized using known methods (Scheme S1, SI) and characterized by various analytical techniques such as ^{1}H NMR, ^{13}C NMR, IR and mass spectroscopy. The solution state UV-vis absorption and emission spectra were recorded in chloroform (Figure S1, SI). Solutions of **OT1** and **OT2** exhibited an absorption at 530 and 508 nm, while emission maximum was at 710 and 684 nm, respectively. The corresponding spin-cast films showed red-shifted absorption

[a] T. Ghosh, N. Raveendran, V. Darshan, Dr. V. C. Nair
Photosciences and Photonics Section
CSIR-National Institute for Interdisciplinary Science and Technology (NIIST)
Thiruvananthapuram 695 019 (India)
.
E-mail: cvijayakumar@niist.res.in

[b] T. Ghosh, Dr. V. C. Nair
Academy of Scientific and Innovative Research (AcSIR), Ghaziabad 201002 (India)

[c] Dr. S. Nagasawa, Prof. A. Saeki
Department of Applied Chemistry, Graduate School of Engineering, Osaka University
2-1 Yamadaoka, Suita, Osaka 565-0871 (Japan)

Supporting information and the ORCID identification number(s) for the author(s) of this article can be found under:
https://doi.org/10.1002/asia.201900024.

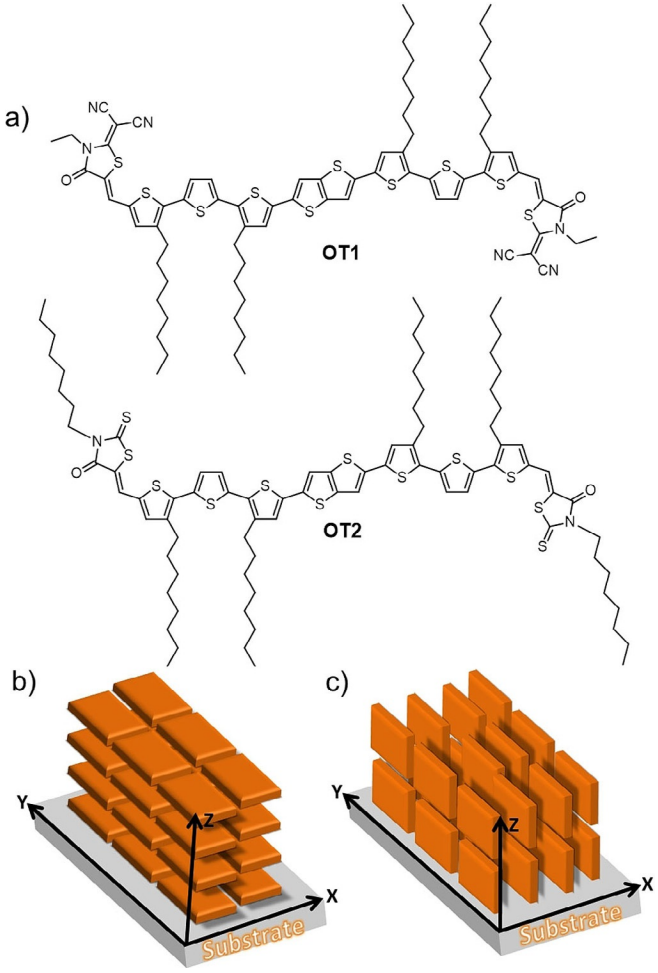

Scheme 1. a) Chemical structure of the thiophene oligomers under study. Schematic illustration of the orientation of respective as-cast oligomers on the substrate; b) **OT1** and c) **OT2**. The arrows represent the X, Y and Z directions of the chromophore packing with respect to the substrate.

maxima (**OT1**: 614 nm and **OT2**: 592 nm, Figure S2, SI) due to the planarization of the conjugated backbone. Films were non-emissive, which could be attributed to the faster non-radiative decay due to the closer interactions of chromophores in the film state. Both solution and film state measurements revealed a bathochromic shift in the absorption of **OT1** when compared to that of **OT2** emphasizing the presence of a stronger acceptor in the former. The absorption spectrum of both oligomers was measured in a "poor" solvent (methylcyclohexane) and compared it with that in a "good" solvent (chloroform), which revealed the self-assembly behavior of the oligomers (Figure S3, SI). The electrochemical properties of the oligomers in the film state were characterized by cyclic voltammetry (CV) using Fc/Fc^+ redox couple as an external standard (Figure S4 and Table S1, SI). The electrochemical band gaps were calculated as 1.64 eV for **OT1** and 1.79 eV for **OT2**; the lower band gap of **OT1** could be attributed to the presence of cyano groups on the rhodanine derivative. Literature reports suggest that the cyano group can reduce the energy level of the LUMO by up to ~0.25 eV.[9a] Since their effect on the HOMO is relatively less, molecules with cyano substitution show a decrease in band gap when compared to that of molecules without cyano group.[9]

2D-Grazing-incidence X-ray diffraction (2D-GIXRD) analysis was carried out to study the packing orientation relative to the substrate, pi-stacking distance and crystallinity of the oligomers.[10] Thin films were prepared by dissolving the oligomers in chloroform and spin-casting over ITO substrate. The scattering angle and scattering vectors (q) in reciprocal space were collected in two dimensions. The domain sizes and orientations were also extracted. The diffraction patterns and the corresponding 2D images are shown in Figure 1. The d-spacing was determined by the relationship, $d = 2\pi/q$. Notably, the pristine samples of both oligomers have similar π–π stacking distances (3.67 Å for **OT1** and 3.65 Å for **OT2**) implying that the stacking of the molecules is not affected by the differential substitution at the acceptor units. However, their presence has an obvious impact on the orientation of the oligomers on the substrate. In **OT1**, the absence of lamellar stacking peak (at $q_z = 3$–$4\ nm^{-1}$) and a distinct and intense π–π stacking reflection in the out-of-plane direction at $q_z = 17.15\ nm^{-1}$ implies the oligomers are stacked with a face-on orientation. On the other hand, an intense lamellar stacking peak at $q_z = 3.60\ nm^{-1}$ and weak π–π stacking peak at $q_{xy} = 17.20\ nm^{-1}$ was observed for **OT2**, which indicates edge-on orientation of the self-assembled

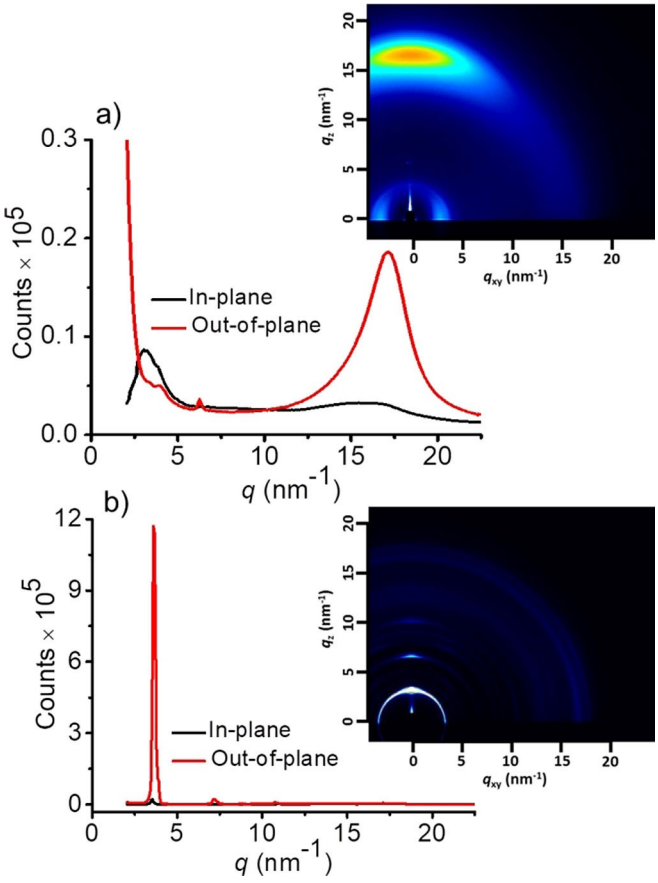

Figure 1. Two-dimensional grazing incidence X-ray diffraction from thin films of a) **OT1** and b) **OT2** in the out-of-plane (red) and in-plane (black) directions. Insets show the corresponding 2D images of the diffraction pattern. The diffraction spectra are extracted from the 2D pattern.

oligomers. The ratio of face-on orientation ($R_{face\text{-}on}$ in %) was evaluated by *I*ip/(*I*ip + *I*op) and edge-on orientation ($R_{edge\text{-}on}$ in %) was calculated by *I*op/(*I*ip + *I*op), where *I*ip and *I*op are the peak intensities of (100) diffraction in the in-plane and out-of-plane directions, respectively. From the graph, we have extracted $R_{face\text{-}on}$ as 89% for **OT1** and $R_{edge\text{-}on}$ as 98% for **OT2**.

Herman's orientation parameter (*S*) was calculated based on the (100) diffraction along the azimuthal arch (0–90°), where $S = -0.5$, 0 and 1 represent a perfect face-on, random orientation, and perfect edge-on orientation, respectively.[11] **OT1** and **OT2** exhibit the '*S*' of −0.15 and 0.41, which are high-score face-on and edge-on orientations, respectively (Figure S5, SI). It could be assumed that the alkyl chains on the end groups played a key role on the supramolecular assembly of the oligomers on the substrate. Presence of equally long alkyl chains on either side (octyl on thiophene and nitrogen atom of rhodanine) supported **OT2** to stand on the substrate yielding edge-on orientation. On the other hand, the presence of unsymmetrical alkyl chains (octyl on thiophene and ethyl on the nitrogen atom of rhodanine) can't provide such support in **OT1** resulting in the oligomer assembly to fall on the substrate yielding face-on orientation. Though the dicyano groups in **OT1** provide larger π-surface and facilitate π–π stacking of chromophores, their role on the preferential orientation on the substrate is not clear from our studies.

The AFM images of drop cast samples showed disparity in the film microstructure between oligomers on ITO substrate portraying its difference in preferential stacking. The topography of **OT1** film revealed a featureless or amorphous nature (Figure 2a) with root-mean-square roughness of 2.97 nm, whereas, **OT2** displayed leaf-like morphology (Figure 2b) with a larger roughness of 10.49 nm, presumably due to its stronger crystallinity as reflected in GIXRD. In other words, the obtained morphologies support a picture in which the face-on domains percolate throughout the whole substrate surface without any significant features, while edge-on domains result in structural variations in the bulk of the material due to the lateral growth of stacks. The cross-sectional analysis of the AFM images revealed that the average height of the aggregates of **OT1** is ~15 nm (Figure 2c), and that of **OT2** is ~55 nm (Figure 2d). Interestingly, these morphological features are independent of substrate nature as evident from the observation of similar morphologies on gold (Figure S6, SI) and SiO_2 (Figure S7, SI) substrates. This indicates that the key steps in the self-assembly process happen in the presence of the solvent and the substrate has a negligible effect on it.

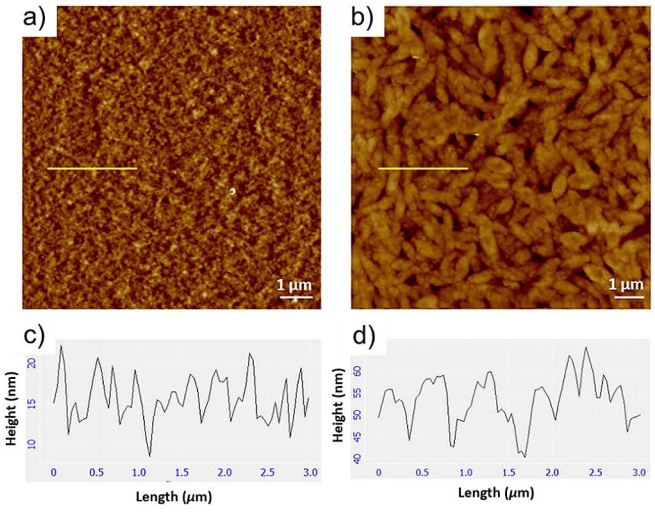

Figure 2. AFM height images of a) **OT1** and b) **OT2** on ITO drop-cast from chloroform solution. c) and d) show the corresponding cross-sectional analysis (the selected area is indicated by a yellow line on the image).

It is a well-known fact that the surface-enhanced Raman spectroscopy (SERS) signals get amplified when a Raman active molecule is in close proximity with gold or silver nanoparticles.[12] In order to reiterate the differential orientation, we analysed the Raman signals of the oligomers on a SERS substrate under identical conditions. For this purpose, SERS substrates consisting of gold nanoparticles of an average diameter of 20 nm (Figure S8, SI) were prepared. Chloroform solutions of the molecules were drop-cast over the substrates and dried under vacuum. The Raman spectra of oligomers on SERS and glass (for comparison purpose) substrates were recorded on excitation with 633 nm laser (Figure 3). A prominent signal was

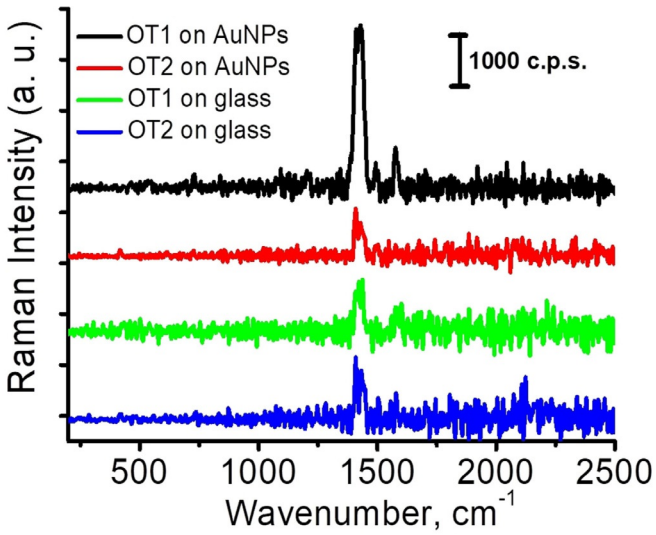

Figure 3. Raman spectra of **OT1** and **OT2** on gold nanoparticles (AuNPs) and glass substrates. A film of gold nanoparticles of an average diameter of 20 nm was used as the SERS substrate.

obtained at 1410 cm^{-1}, which corresponds to the C=C symmetric stretching mode of thiophene ring. Interestingly, 3-fold enhancement of the signal was observed for **OT1** on the SERS platform when compared to that on the glass. However, no such enhancement was seen in the case of **OT2**. It must be noted that the enhancement of Raman signals depends on a number of factors; one major reason among them is the orientation of chromophores on the nanoparticle surface. Since **OT1** is face-on to the substrate, the pi-conjugated chromophores interact more efficiently with the SERS substrate, which can generate a good number of hotspots and produce an enhanced electromagnetic field, leading to signal enhancement.

While in the case of **OT2**, as it is edge-on to the substrate, the chromophores are not in a position to effectively interact with gold nanoparticles and hence resulting in weaker signals only. This observation is in good agreement with the GIXRD and AFM analysis.

Charge transport is highly anisotropic in well-ordered pi-conjugated molecules and current flow is usually high in the pi-stacking direction because of maximal overlap of orbitals occurs in that direction, which in turn favour maximum charge transport. Since **OT1** and **OT2** stack differently on substrates, the conductivity is expected to be different in orthogonal directions. To validate this point, conducting-atomic force microscopy (c-AFM) experiment was performed on the oligomers under ambient conditions. For this purpose, the oligomers were allowed to self-assemble on FET type substrates (gold electrode deposited on half of the SiO_2 through vacuum deposition) by drop-casting from chloroform solution. The drop cast on the substrates was done in such a way that half of the sample was on the gold electrode and the remaining half on SiO_2. The current was measured both vertically and horizontally by varying the position of AFM tip/electrode contacts. The measurement set-up is represented schematically in Figure 4a. The drop cast samples of both oligomers have a thickness of about 70 nm. In the case of **OT1**, when the AFM tip was kept on the sample at position A, that is, the sample is vertically above the gold electrode, it showed a conductivity of $1.45\times10^{-1}\,Sm^{-1}$ (Figure 4b). On the other hand, when the tip was at position B, the conductivity was about three order less ($1.32\times10^{-4}\,Sm^{-1}$). The lower conductivity at position B could be attributed to the unfavorable charge transport in this direction. On the other hand, in the case of **OT2**, high conductivity was observed in the horizontal direction (position B; $2.34\times10^{-2}\,Sm^{-1}$; Figure 4c), while lower conductivity was measured at position A ($1.96\times10^{-4}\,Sm^{-1}$). About 15 scans were performed to check the repeatability and the obtained results were averaged. Hence, this experiment unambiguously proved that the differential packing orientation of **OT1** and **OT2** is not only reflected on the morphological features but also on the functional property such as charge transport.

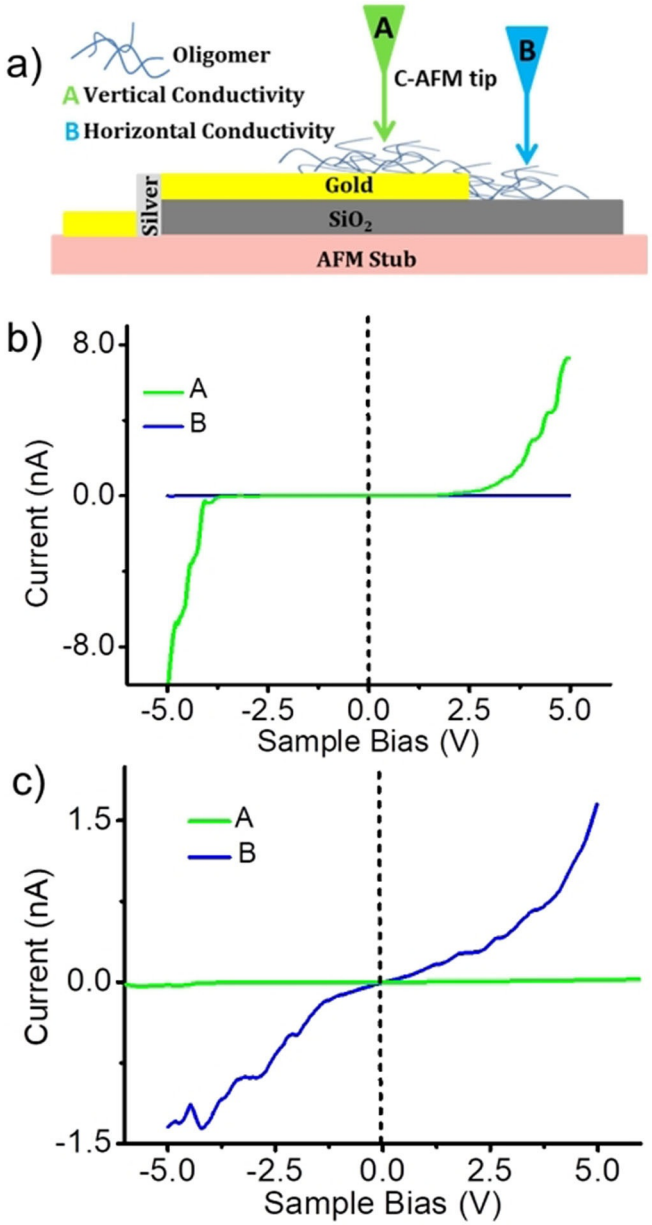

Figure 4. a) Schematic representation of the c-AFM measurement set-up. *I-V* curves of b) **OT1** and c) **OT2** assemblies, measured at positions indicated by 'A' and 'B' on the substrate using an AFM tip of radius 25 nm, between +5 V to −5 V with an applied bias voltage of 500 mV.

In summary, our studies revealed that rational functionalization of semiconducting thiophene oligomers results in preferential orientation of the conjugated backbone on the surface of various substrates induced by differential self-assembly. The alkyl chains on the thiophene backbone and rhodanine end-groups played a key role in the chromophore orientation in the film state. Such supramolecular control over the chromophore packing helps to tune the direction of charge carrier transport in organic semiconductors, which is helpful for developing efficient photovoltaic and thin-film transistor devices.

Experimental Section

Detailed experimental information is provided in the Supporting Information.

Acknowledgements

This work was financially supported by DST through the Ramanujan Fellowship (SR/S2/RJN-133/2012). T.G. is grateful to UGC for the Senior Research Fellowship. The authors thank Dr. Kaustabh Kumar Maiti and Jyothi B. Nair for Raman studies and Dr. Tomoyuki Koganezawa at JASRI, Japan and Dr. Itaru Osaka at Hiroshima University, Japan, for the 2D-GIXRD experiments.

Conflict of interest

The authors declare no conflict of interest.

Keywords: anisotropic conductivity · donor-acceptor systems · grazing incidence X-ray diffraction · organic semiconductors · self-assembly

[1] a) J. R. Tumbleston, B. A. Collins, L. Yang, A. C. Stuart, E. Gann, W. Ma, W. You, H. Ade, *Nat. Photonics* **2014**, *8*, 385 – 391; b) H. Sirringhaus, *Adv. Mater.* **2014**, *26*, 1319 – 1335; c) M. J. Sung, A. Luzio, W. T. Park, R. Kim, E. Gann, F. Maddalena, G. Pace, Y. Xu, D. Natali, C. de Falco, L. Dang, C. R. McNeill, M. Caironi, Y. Y. Noh, Y. H. Kim, *Adv. Funct. Mater.* **2016**, *26*, 4984 – 4997; d) H. Lee, D. Lee, D. H. Sin, S. W. Kim, M. S. Jeong, K. Cho, *NPG Asia Mater.* **2018**, *10*, 469 – 481; e) O. A. Ibraikulov, C. Ngov, P. Chavez, I. Bulut, B. Heinrich, O. Boyron, K. L. Gerasimov, D. A. Ivanov, S. Swaraj, S. Mery, N. Leclerc, P. Leveque, T. Heiser, *J. Mater. Chem. A* **2018**, *6*, 12038 – 12045; f) C. Wang, H. Nakamura, H. Sugino, K. Takimiya, *J. Mater. Chem. C* **2018**, *6*, 3604 – 3612; g) S. Feng, C. Zhang, Z. Bi, Y. Liu, P. Jiang, S. Ming, X. Xu, W. Ma, Z. Bo, *ACS Appl. Mater. Interfaces* **2019**, *11*, 3098 – 3106.

[2] a) R. Rieger, D. Beckmann, A. Mavrinskiy, M. Kastler, K. Müllen, *Chem. Mater.* **2010**, *22*, 5314 – 5318; b) M. S. Chen, J. R. Niskala, D. A. Unruh, C. K. Chu, O. P. Lee, J. M. J. Fréchet, *Chem. Mater.* **2013**, *25*, 4088 – 4096; c) L. Yang, S. Zhang, C. He, J. Zhang, Y. Yang, J. Zhu, Y. Cui, W. Zhao, H. Zhang, Y. Zhang, Z. Wei, J. Hou, *Chem. Mater.* **2018**, *30*, 2129 – 2134.

[3] a) S. Guo, E. M. Herzig, A. Naumann, G. Tainter, J. Perlich, P. Müller-Buschbaum, *J. Phys. Chem. B* **2014**, *118*, 344 – 350; b) T. Ghosh, A. Gopal, S. Nagasawa, N. Mohan, A. Saeki, V. C. Nair, *ACS Appl. Mater. Interfaces* **2016**, *8*, 25396 – 25404.

[4] a) C. McDowell, M. Abdelsamie, M. F. Toney, G. C. Bazan, *Adv. Mater.* **2018**, *30*, 1707114; b) W. Wang, L. Song, D. Magerl, D. M. González, V. Körstgens, M. Philipp, J. Moulin, P. Müller-Buschbaum, *Adv. Funct. Mater.* **2018**, *28*, 1800209.

[5] a) P. Dhar, P. P. Khlyabich, B. Burkhart, S. T. Roberts, S. Malyk, B. C. Thompson, A. V. Benderskii, *J. Phys. Chem. C* **2013**, *117*, 15213 – 15220; b) S. Grob, A. N. Bartynski, A. Opitz, M. Gruber, F. Grassl, E. Meister, T. Linderl, U. Hörmann, C. Lorch, E. Moons, F. Schreiber, M. E. Thompson, W. Brütting, *J. Mater. Chem. A* **2015**, *3*, 15700 – 15709; c) G. L. Schulz, M. Lobert, I. Ata, M. Urdanpilleta, M. Lind, A. Mishra, P. Bäuerle, *J. Mater. Chem. A* **2015**, *3*, 13738 – 13748.

[6] X. Zhang, L. J. Richter, D. M. Delongchamp, R. J. Kline, M. R. Hammond, I. McCulloch, M. Heeney, R. S. Ashraf, J. N. Smith, T. D. Anthopoulos, B. Schroeder, Y. H. Geerts, D. A. Fischer, M. F. Toney, *J. Am. Chem. Soc.* **2011**, *133*, 15073 – 15084.

[7] S. Subramaniyan, H. Xin, F. S. Kim, S. Shoaee, J. R. Durrant, S. A. Jenekhe, *Adv. Energy Mater.* **2011**, *1*, 854 – 860.

[8] a) I. Osaka, T. Kakara, N. Takemura, T. Koganezawa, K. Takimiya, *J. Am. Chem. Soc.* **2013**, *135*, 8834 – 8837; b) I. Osaka, M. Saito, T. Koganezawa, K. Takimiya, *Adv. Mater.* **2014**, *26*, 331 – 338.

[9] a) A. Casey, S. D. Dimitrov, P. Shakya-tuladhar, Z. Fei, M. Nguyen, Y. Han, T. D. Anthopoulos, J. R. Durrant, M. Heeney, *Chem. Mater.* **2016**, *28*, 5110 – 5120; b) F. Glocklhofer, A. J. Morawietz, B. Stoger, M. M. Unterlass, J. Frohlich, *ACS Omega* **2017**, *2*, 1594 – 1600.

[10] a) A. Saeki, M. Tsuji, S. Yoshikawa, A. Gopal, S. Seki, *J. Mater. Chem. A* **2014**, *2*, 6075 – 6080; b) M. A. Adil, J. Zhang, D. Deng, Z. Wang, Y. Yang, Q. Wu, Z. Wei, *ACS Appl. Mater. Interfaces* **2018**, *10*, 31526 – 31534; c) D. Chiou, Y. Su, K. Hung, J. Hsu, T. Hsu, T. Wu, Y. Cheng, *Chem. Mater.* **2018**, *30*, 7611 – 7622.

[11] a) A. L. Perez, P. Zalar, L. Ying, K. Schmidt, M. F. Toney, T. Nguyen, G. C. Bazan, E. J. Kramer, *Macromolecules* **2014**, *47*, 1403 – 1410; b) M. Ide, A. Saeki, *Chem. Lett.* **2017**, *46*, 1133 – 1136.

[12] N. D. Israelsen, C. Hanson, E. Vargis, *Sci. World J.* **2015**, *2015*, 124582.

Manuscript received: January 6, 2019
Revised manuscript received: February 8, 2019
Accepted manuscript online: February 12, 2019
Version of record online: March 5, 2019